UNIVERSITY OF BIRMINGHAM
University of Birmingham Research at Birmingham

Interaction networks, ecological stability, and collective antibiotic tolerance in polymicrobial infections

de Vos, Marjon; Zagorski, Marcin; McNally, Alan; Bollenbach, Tobias

DOI:
10.1073/pnas.1713372114

License:
None: All rights reserved

Document Version
Peer reviewed version

Citation for published version (Harvard):
de Vos, M, Zagorski, M, McNally, A & Bollenbach, T 2017, 'Interaction networks, ecological stability, and collective antibiotic tolerance in polymicrobial infections', *National Academy of Sciences. Proceedings*, vol. 114, no. 40, pp. 10666-10671. https://doi.org/10.1073/pnas.1713372114

Link to publication on Research at Birmingham portal

General rights
Unless a licence is specified above, all rights (including copyright and moral rights) in this document are retained by the authors and/or the copyright holders. The express permission of the copyright holder must be obtained for any use of this material other than for purposes permitted by law.

• Users may freely distribute the URL that is used to identify this publication.
• Users may download and/or print one copy of the publication from the University of Birmingham research portal for the purpose of private study or non-commercial research.
• User may use extracts from the document in line with the concept of 'fair dealing' under the Copyright, Designs and Patents Act 1988 (?)
• Users may not further distribute the material nor use it for the purposes of commercial gain.

Where a licence is displayed above, please note the terms and conditions of the licence govern your use of this document.

When citing, please reference the published version.

Take down policy
While the University of Birmingham exercises care and attention in making items available there are rare occasions when an item has been uploaded in error or has been deemed to be commercially or otherwise sensitive.

If you believe that this is the case for this document, please contact UBIRA@lists.bham.ac.uk providing details and we will remove access to the work immediately and investigate.

Download date: 26. Aug. 2022

Interaction networks, ecological stability, and collective antibiotic tolerance in polymicrobial infections

Short title: Ecological interactions in polymicrobial infections

Authors: M.G.J. de Vos[1,2], M. Zagorski[2], A. McNally[3], T. Bollenbach[2,4]*

Affiliations:
[1] Wageningen University, Laboratory of Genetics, Wageningen, The Netherlands.

[2] IST Austria, Klosterneuburg, Austria.

[3] University of Birmingham, Institute of Microbiology and Infection, Birmingham, United Kingdom.

[4] University of Cologne, Institute of Theoretical Physics, Cologne, Germany.

*Correspondence to: t.bollenbach@uni-koeln.de

BIOLOGICAL SCIENCES: Biophysics and Computational Biology, Ecology, Systems Biology, Microbiology

Abstract

Polymicrobial infections constitute small ecosystems that accommodate several bacterial species. Commonly, these clinical isolates are investigated in isolation. It is however unknown to what extent the isolates in these communities interact and whether their interactions alter bacterial growth and ecosystem resilience in the presence and absence of antibiotics. We quantified the complete ecological interaction network for 72 bacterial isolates collected from 23 individuals diagnosed with polymicrobial urinary tract infections (UTIs) and found that most interactions are evolutionarily conserved. Statistical network analysis revealed that competitive and cooperative reciprocal interactions are enriched in the global network, while cooperative interactions are depleted in the individual host-community networks. A population dynamics model parameterized by our measurements suggests that interactions restrict community stability, explaining the observed species diversity of these communities. We further show that the clinical isolates frequently protect each other from clinically relevant antibiotics. Together, these results highlight that ecological interactions are crucial for the growth and survival of bacteria in polymicrobial infection communities and affect their assembly and resilience.

Significance statement

Comment [MdV1]: Max 120 words

In many infections, multiple microbial species are ~~simultaneously~~ present simultaneously ~~at the infection site~~. Such polymicrobial infections can be viewed as small microbial ecosystems. Do bacteria in these communities interact with each other? And if so, do these interactions affect the stability of the ecosystem, in particular when antibiotics are present? ~~Here, we~~We focus on urinary tract infections and demonstrate that there are ample ecological interactions between different bacterial species~~. These interactions occur~~, both in the presence and in the absence of

antibiotics. We further show that they crucially affect ecosystem stability and resilience to environmental perturbations such as antibiotics. Understanding the nature of these polymicrobial communities can point us to ways of disrupting infection ecosystems, which could potentially be used as a new strategy to eradicate infective communities.

Introduction

Bacteria in a polymicrobial infection form an ecosystem that can be more than the sum of its parts. Interactions between microbes can alter the severity of infections (1, 2) and complicate treatments (3–6). Still, the interplay between microbes in clinical environments remains poorly understood, as clinical isolates are commonly investigated in isolation. This leads to the implicit assumption that microorganisms in polymicrobial infections grow and can be treated independently of each other. Ecological interactions occur when organisms affect each other's proliferation or survival. Mechanistically, such interactions can be due to competition for the same nutrient (7), excretion of metabolites (cross-feeding) (8), or production of other molecules that specifically harm or help other community members; the latter include antibiotics (9), bacteriocins (10), phenazines (11), siderophores (12) and signaling molecules (13). The quantitative analysis of ecological interactions between microbes can shed light on the emergent properties of the infection ecosystem, its microbial interaction network (14–17), stability, and resilience to perturbations.

Polymicrobial urinary tract infections (UTIs) in elderly patients consist of relatively simple bacterial communities (Fig. 1A) (6). However, the role of ecological interactions between these bacteria (3, 5) largely remains obscure. As the communities are typically caused by only up to five strains (6), it is feasible to systematically investigate all interactions. This is in contrast to other ecosystems that are generally too complex to map the network of all interactions (15, 18). Due to the lack of comprehensive experimental data on interactions, quantitative studies of microbial ecosystems have so far relied on theoretical modeling (15, 19, 20) sequencing methods (21) or focused on incomplete sub-communities (22). Indeed, only a few studies experimentally

quantified ecological interactions in different microbial ecosystems on a larger scale (22–25). Importantly, these interactions can potentially alter the efficacy of drug treatments as bacteria can protect others from the effect of antibiotics (26), in the simplest case by just degrading the drug (13, 27, 28). Thus, understanding the effects of ecological interactions on bacterial growth and antibiotic efficacy is crucial for elucidating the nature of polymicrobial infections.

To elucidate the role of ecological interactions in polymicrobial infections, independent of their underlying mechanisms, we systematically quantified the entire interaction network between 72 clinical isolates from polymicrobial UTIs in the absence and presence of clinically relevant antibiotics. We found that isolates commonly compete with each other while cooperation occurs to a lesser extent. Using a theoretical model parameterized by our measurements we found that interactions restrict community stability, explaining the observed community size. Interactions further lead to collective drug tolerance: bacteria tend to protect each other from antibiotics with the most sensitive strains being protected the most. These results highlight the importance of microbial interactions for understanding polymicrobial infections and suggest new treatment strategies aimed at the entire community, not at individual pathogens.

Results

Systematic quantification of ecological interactions between isolates from polymicrobial UTIs reveals many positive and negative interactions

We systematically quantified all pair-wise interactions between 72 bacterial strains isolated from 23 elderly persons showing symptoms of UTI which cultured polymicrobial communities. Each community isolated from the same host contained 4-5 distinct strains (Fig. 1A, SI Methods) (6).

To identify key ecological properties of polymicrobial communities we used a high-throughput approach; we measured the maximum growth yield (optical density) and the growth rate of all isolates in artificial urine medium. The medium was conditioned by growing single isolates for 48 hours, recovering the supernatant, and replenishing it with nutrients (Fig. 1B, SI Methods). We quantified interactions using the parameter $\varepsilon=\log(N_c/N_u)$; here, N_c and N_u are the growth yield in conditioned and in unconditioned medium, respectively; growth rate interactions are described analogously. Thus, a positive interaction ($\varepsilon>0$) corresponds to an increase in growth compared to the reference medium (e.g. due to cross-feeding) and a negative interaction ($\varepsilon<0$) to a decrease (e.g. due to niche overlap) (Fig.1 C,D).

We observed many positive and negative interactions between isolates from polymicrobial UTIs. Using a stringent threshold for detecting significant interactions (SI Methods) most interactions were neutral but 18% of all possible interactions were positive and nearly 40% of these led to a >2-fold increase in growth yield (Fig. S1, $\varepsilon>0.7$). Similarly, 23% of all possible interactions were negative; most of these (78%) were relatively weak ($\log(0.6)=-0.51>\varepsilon>\log(0.8)=-0.22$, Fig. S1). The frequent occurrence of interactions highlights the limitations of investigating individual strains in isolation when tackling polymicrobial infections.

Interactions are largely determined by phylogeny

Statistical analysis of the global network of ecological interactions revealed key features of interspecific relationships. Clustering the strains by phylogenic distance (SI Methods) exposed that the interactions between pairs of strains are largely determined by their respective genera as the phylogenetic clusters coincide with similarly clustered interactions in the interaction matrix (Fig. 2A,B, Fig. S2). This observation supports the view that these ecological interactions cluster

based on evolutionary relatedness (29). Within-genus interactions are predominantly negative or neutral (Fig. 2B, Fig. S3, Table S1), consistent with the paradigm that closely related strains tend to have negative interactions, often due to niche overlap (30). Among the clearest features in the interaction network is that enterococci and staphylococci benefit from many other genera but mostly do not affect the others in return (Fig. 2B). In contrast, *Proteus mirabilis* affects many other genera negatively and is also often negatively affected by others, confirming previous reports (31). Few individual strains display interactions that deviate from the general trends for the genera (Fig. 2A,B, Fig. S2). Hence, these data support that most ecological interactions in these polymicrobial communities are evolutionarily conserved. This suggests that despite the high potential for genotypic diversity within these groups, these ecological interactions are deep-branching, and possibly ancestral.

The interaction strength distributions differ qualitatively between the genera. Specifically, the strength distribution of outgoing negative interactions is either unimodal, peaking between $\varepsilon=\log(1)=0$ and $\varepsilon\approx\log(0.8)=-0.22$, and dropping to zero around $\varepsilon\approx\log(0.6)=-0.51$ (for *Escherichia coli*, *Staphylococcus*, *Klebsiella*, *Enterobacter*, *Citrobacter*), or it is bimodal with a second peak near zero (for *Proteus mirabilis* and *Pseudomonas*; Fig. S4). The interaction parameter $\varepsilon=\log(0.6)$ corresponds to complete niche overlap while lower values indicate active growth inhibiting mechanisms (SI Methods).

Reciprocal interactions, in particular competition, are enriched in the interaction network

It is a fundamental question if microbes in polymicrobial infections predominantly cooperate or compete with each other (4). To systematically identify such interaction patterns between pairs of strains, we compared the occurrence of two-node subnetworks in the measured interaction

network to that in an ensemble of randomized measured networks that preserve the degree distribution (SI, Methods). This analysis revealed that reciprocal interactions are generally enriched: competitive (-/-) and cooperative (+/+) interactions are significantly overrepresented in the measured network (-/-, z-score 4.76, $p < 10^{-5}$; +/+, z-score 2.70, $p = 0.007$, Fig. 2C, SI Methods) – an interesting similarity to *Streptomyces* communities in soil (23). The enrichment of competitive interactions supports the general predominance of competitive interactions in ecosystems (22). In addition, exploitive (+/-) interactions are extremely underrepresented (z-score -6.13, $p < 10^{-9}$, Fig. 2C) (SI Methods). Mutual interactions within each genus are generally enriched for competition and amensalism and depleted of cooperation and commensalism (Fig. S8, Table S1), supporting the paradigm that competition is the dominant interaction type between closely related strains (32, 33); the sole exception is *Staphylococcus* (Fig. S3, Table S1). Overall, this analysis shows that predominance of reciprocal interactions, in particular competition, is a hallmark of the polymicrobial UTI ecosystem.

Communities are more enriched for competition

We next asked if the strains derived from each host were selected based on their ecological interactions with other community members or if the host community is a random assembly of strains, reflecting chance invasion events of UTI strains, mostly from the gut (34). At odds with the latter scenario, the distribution of genera in the communities derived from individual hosts was not random: enterococci and *E. coli* occurred together significantly more frequently than expected at random ($p=0.004$, Fig. S5A, SI Methods), in accordance with previous reports (35). Compared to random strain assemblies, the complete host communities further tended to be enriched for negative interactions (Fig. S5B) and competition, and depleted of exploitation and cooperation (Fig. 3A,B, SI Methods). These trends for increased competition in communities

from the same site are opposite to those for *Streptomyces* communities on soil grains (23) but consistent with findings on *Baccillus* spp from lagoons (25) and the microbiome (15). The predominance of competitive interactions between coexisting strains in UTIs defies the naïve expectation that bacteria in these communities are selected based on their ability to cooperate.

Most communities are ecologically stable but can be destabilized by targeted invaders

To elucidate the underlying principles and dynamics of UTI community assembly, we next investigated the ecological stability of the communities. To this end, we generalized an ecological logistic growth model to capture interactions at the level of both growth rate and yield (SI Methods). All parameters entering this model are constrained by our comprehensive quantitative interaction data (Fig. 2A). For simplicity, we assumed that interactions are additive when more than two strains are present. This model thus provides a theoretical description of population dynamics in polymicrobial communities and makes quantitative predictions for the stability and dynamics of arbitrary assemblages of strains.

UTI communities from the same host are often stable and can assemble in any order. We found that 4 out of 8 complete communities consisting of four different strains have at least one stable fixed point (attractor) in which all strains co-exist, whereas the other 4 communities do not allow for stable coexistence (Fig. 3C, SI Methods). The presence of a single attractor in which all strains co-exist implies that the community is resilient: it returns to this attractor and thus maintains co-existence even upon large perturbations e.g. caused by a short antibiotic treatment. The fraction of communities that allow for stable co-existence is not significantly different from that of randomly assembled communities (Fig. 3D, p~0.9, 1,000 sets of 8 randomly assembled communities, SI Methods). While most stable communities can be assembled strain-by-strain in

any order (i.e. all intermediate communities are stable), 1 of the 4 communities that allow for stable co-existence had an additional unstable fixed point. This implies that some assembly orders are excluded, as they lead to the loss of at least one community member. Overall, these results suggest that many possible combinations of UTI isolates could in principle form stable communities.

It is of key relevance for probiotic treatments if stable communities can be invaded and potentially destabilized by newly arriving strains. We thus described invasion attempts by adding a few individuals of an invading strain and calculated the ensuing community dynamics. We found that many randomly chosen invading UTI strains can coexist with the host community (on average 45%), but for a considerable fraction (~30%) one of the original strains is replaced by the invader. About 15% of invasion attempts fail, resulting in the loss of the invader. And in less than 10% of cases the invader can destabilize the community, leading to the loss of more than one community member (Table S2). Thus, invaders are often incorporated in the community or switch sides with community members, suggesting that UTI communities are dynamically stable.

The typical community size is close to the maximum that allows for stability

Our ecological model makes a prediction for the maximum size of a stable UTI community. The relation between stability and community size is at the heart of a long-standing debate (17, 36). Testing the stability of communities with an increasing number of randomly chosen UTI strains (SI Methods), we found a transition from stability to instability around a community size of 4-5 strains (Fig. 3D). For 5 strains, the fraction of stable communities was below 25% and rapidly decayed further, falling below 2% at community size 8 (Fig. 3D). This typical community size of

4-5 strains predicted from the model agrees with the number of different strains isolated from polymicrobial UTIs (6) and suggests that larger communities are unsustainable.

Community stability also depends on the voiding and refilling of the bladder which removes and effectively dilutes the UTI strains. When this effect is included in the ecological model, all strains are washed out if the effective dilution rate exceeds a critical value (37) (SI Methods). In our model, *E. coli* is consistently among the last two strains that can still persevere at the highest dilution rates (Fig. 3E, Fig.S6). For lower dilution rates, communities with an increasing number of different strains are stably maintained. This effect can explain the higher incidence of polymicrobial UTIs in elderly men who have an increased bladder "dead volume" which effectively reduces the dilution rate (Fig. 3E, Fig. S6, SI Methods)(38) and contributes to shifting the female versus male incidence ratio from 30:1 to 2:1 in the elderly (39). Indeed, using plausible estimates for the effective dilution rate in our model, infections in individuals with urinary retention allow for stable co-existence of polymicrobial communities while those in healthy individuals tend to be clonal (Fig. 3E, Fig. S6, SI Methods). Overall, these results support that ecological interactions and dilution together determine the stability of polymicrobial communities and constrain their maximum size.

Bacterial interactions affect antibiotic tolerance

The fact that UTIs are often treated with antibiotics (40) raises the question if ecological interactions alter the efficacy of antibiotics. We therefore measured the effects of media conditioned by 14 different donor strains on all 72 acceptor strains in the presence of two different antibiotics that are commonly used for the treatment of UTIs: trimethoprim-sulfamethoxazole (41, 42) and nitrofurantoin (43). The donor strains were selected to represent

the diversity of the genera in our dataset. We assessed the fold-change in antibiotic tolerance by comparing the concentrations of antibiotics that sustained growth in the conditioned medium and the unconditioned reference (Fig. 4 A,B, Fig. S6A, SI Methods).

The clinical isolates often protect each other from antibiotics. We observed >3.5-fold increases in the tolerance to trimethoprim-sulfamethoxazole for 25% of tested interactions but decreases of the same magnitude in only 12% of cases (Fig. 4A, Fig. S7A); this trend was similar for nitrofurantoin (18% and 8%, respectively; Fig. 4B, Fig. S7A). The protection effects were often correlated with positive interactions in the absence of antibiotics. However 13% of the protective interactions for trimethoprim-sulfamethoxazole were neutral in the absence of antibiotics, whereas for nitrofurantoin 9% of these protective interactions were 'silent' in the environment without antibiotics (Fig. S7B,C). Notably, the protective effect on *Enterococcus* spp and *Staphylococcus* spp corresponds with their positive incoming interactions in the absence of antibiotics (Fig. 2B, 4C, S8). Interestingly, *Enterococcus* spp returned the favor by decreasing the antibiotic tolerance of several other strains (Fig. 4C, S8). *Proteus mirabilis* predominantly protected other strains from antibiotics (Fig. 4C, S8), while this species mostly harmed others in the absence of antibiotics (Fig. 2B). As *Proteus mirabilis* produces ammonia and increases the pH of the medium, its protective effect is consistent with reports that ammonia and an increased pH in the environment decrease the efficacy of antibiotics (44–46). We further found that drug tolerance increased more strongly the less resistant the strain was to the drug (Pearson's ρ=-0.25 for trimethoprim-sulfamethoxazole and ρ=-0.33 for nitrofurantoin, $p<0.01$ for both antibiotics) and the increase in tolerance to both antibiotics was correlated (ρ=0.24, $p<0.01$). Thus, UTI communities exhibit hallmarks of collective drug tolerance (28, 47): the presence of community

members tends to protect other strains from antibiotics with the most sensitive strains experiencing the greatest benefit.

Communities may be assembled such that collective antibiotic tolerance is boosted. We found that strains from the same community tend to protect each other slightly more frequently from antibiotics than others, while the fraction of interactions that increase antibiotic sensitivity is smaller within communities than between communities (Fig. S7D, SI Methods). Taken together, these data show that ecological interactions affect the growth and survival of the community members in the absence and presence of antibiotics.

Discussion

We elucidated the ecological interaction network of bacteria from elderly persons diagnosed with polymicrobial urinary tract infections. In contrast to e.g. the gut microbiome (15), the UTI community size is relatively small (6) and the strains are readily cultured in the laboratory. This enabled us to measure all pair-wise interactions within these infection communities, and establishes polymicrobial communities as a fruitful and relatively simple model system that enables a uniquely quantitative approach to elucidating key principles of ecology.

Understanding the ecology of polymicrobial interactions may provide opportunities for new treatment strategies. Specifically, we found that UTI communities can be destabilized by a targeted invader strain, although the odds of destabilization are smaller than coexistence of the invader in the community. Quantitative measurements of ecological interaction networks and

ecological models as presented here may therefore guide the design of synthetically modified strains that can destabilize the infection community (48).

Although our standardized high-throughput measurements allowed us to investigate the bacterial interactions in great detail, this study has the general limitations of any reductionist approach in that it cannot capture the full complexity of the host environment. Specifically, the composition of the host's urine can vary in time and between hosts (49); it will thus deviate from our standardized artificial urine medium. In addition, as donor and acceptor bacteria were not in physical contact in our assay, additional contact-mediated interactions (50) may affect *in vivo* interactions. Moreover, higher-order interactions between more than two bacteria could potentially affect community stability (19). However, a recent study found that pair-wise interactions largely predict the population dynamics of larger communities (51). *In vivo*, UTIs could be further complicated by host-pathogen interactions (52, 53), and the micro-biogeography (54, 55); specifically, bacteria may attach to or invade the bladder lining (40). Future studies are needed to investigate these additional factors that can affect bacterial interactions in the host and illuminate the underlying molecular mechanisms, in particular by identifying the molecules excreted by the different bacteria. To shed light on whether the interactions between bacteria derived from polymicrobial infections are preserved *in vivo* and on the additional contributions from interactions between host and microbes, an exciting challenge will therefore be to extend this ecological approach to *in vivo* models of UTIs and other polymicrobial infections. In conclusion, this work shows that polymicrobial infective communities can and should be viewed as small ecosystems, as the emergent properties in these ecosystems can dictate the growth and survival of the individual bacterial community members.

References

1. Arndt WF, Ritts RE (1961) Synergism between staphylococci and *Proteus* in mixed infection. *Exp Biol Med* 108:166–169.
2. Byrd AL, Segre JA (2016) Adapting Koch's postulates. *Science* 351(6270):224–226.
3. Peters BM, Jabra-Rizk MA, O'May G, William Costerton J, Shirtliff ME (2012) Polymicrobial interactions: impact on pathogenesis and human disease. *Clin Microbiol Rev* 25(1):193–213.
4. Short FL, Murdoch SL, Ryan RP (2014) Polybacterial human disease: the ills of social networking. *Trends Microbiol* 22(9):508–516.
5. Brogden KA, Guthmiller JM, Taylor CE (2005) Human polymicrobial infections. *Lancet* 365(9455):253–255.
6. Croxall G, et al. (2011) Increased human pathogenic potential of *Escherichia coli* from polymicrobial urinary tract infections in comparison to isolates from monomicrobial culture samples. *J Med Microbiol* 60(1):102–109.
7. Fredrickson G, Stephanopoulos G (1981) Microbial competition. *Science* 213(4511):972–979.
8. Wintermute EH, Silver PA (2010) Emergent cooperation in microbial metabolism. *Mol Syst Biol* 6:407.
9. Abrudan MI, et al. (2015) Socially mediated induction and suppression of antibiosis during bacterial coexistence. *Proc Natl Acad Sci U S A* 112(35):11054–11059.
10. Riley MA, Wertz JE (2002) Bacteriocin diversity: ecological and evolutionary perspectives. *Biochimie* 84(5–6):357–64.
11. Price-Whelan A, Dietrich LEP, Newman DK (2006) Rethinking "secondary" metabolism: physiological roles for phenazine antibiotics. *Nat Chem Biol* 2(2):71–8.

12. Breum Andersen S, Marvig R, Molinm S, Krogh Johansen H, Griffin A (2015) Long-term social dynamics drive loss of function in pathogenic bacteria. *Proc Natl Acad Sci U S A* 112(34):10756–10761.

13. Lee HH, Molla MN, Cantor CR, Collins JJ (2010) Bacterial charity work leads to population-wide resistance. *Nature* 467(7311):82–85.

14. Yurtsev E., Conwilla A, Gore J (2016) Oscillatory dynamics in a bacterial cross-protection mutualism. *Proc Natl Acad Sci U S A* 113(22):6236–6241.

15. Coyte KZ, Schluter J, Foster KR (2015) The ecology of the microbiome: networks, competition, and stability. *Science* 350(6261):663–666.

16. Widder S, et al. (2016) Challenges in microbial ecology: building predictive understanding of community function and dynamics. *ISME J* 10(11):1–12.

17. May RM (1973) *Stability and complexity in model ecosystems.* (Princeton University Press, New York)

18. Costello EK, Stagaman K, Dethlefsen L, Bohannan BJM, Relman D (2012) The application of ecological theory toward an understanding of the human microbiome. *Science* 336(6086):1255–62.

19. Kelsic ED, Zhao J, Vetsigian K, Kishony R (2015) Counteraction of antibiotic production and degradation stabilizes microbial communities. *Nature* 521(7553):516–519.

20. Czaran T, Hoekstra RF (2009) Microbial communication, cooperation and cheating: quorum sensing drives the evolution of cooperation in bacteria. *PLoS One* 4(8):e6655.

21. Zhernakova A, et al. (2016) Population-based metagenomics analysis reveals markers for gut microbiome composition and diversity. *Science* 352(6285):565–569.

22. Foster KR, Bell T (2012) Competition, not cooperation, dominates interactions among

culturable microbial species. *Curr Biol* 22(19):1845–50.

23. Vetsigian K, Jajoo R, Kishony R (2011) Structure and evolution of *Streptomyces* interaction networks in soil and in silico. *PLoS Biol* 9(10):e1001184.
24. Aguirre-von-Wobeser E, et al. (2014) Two-role model of an interaction network of free-living γ-proteobacteria from an oligotrophic environment. *Environ Microbiol* 16(5):1366–1377.
25. Pérez-Gutiérrez R-A, et al. (2013) Antagonism influences assembly of a *Bacillus* guild in a local community and is depicted as a food-chain network. *ISME J* 7(3):487–497.
26. Vega NM, Allison KR, Samuels AN, Klempner MS, Collins JJ (2013) *Salmonella typhimurium* intercepts *Escherichia coli* signaling to enhance antibiotic tolerance. *Proc Natl Acad Sci U S A* 110(35):14420–14425.
27. Yurtsev EA, Chao HX, Datta MS, Artemova T, Gore J (2013) Bacterial cheating drives the population dynamics of cooperative antibiotic resistance plasmids. *Mol Syst Biol* 9(683):683.
28. Meredith HR, Srimani JK, Lee AJ, Lopatkin AJ, You L (2015) Collective antibiotic tolerance: mechanisms, dynamics and intervention. *Nat Chem Biol* 11(3):182–8.
29. Gómez JM, Verdú M, Perfectti F (2010) Ecological interactions are evolutionarily conserved across the entire tree of life. *Nature* 465(7300):918–21.
30. Hibbing ME, Fuqua C, Parsek MR, Peterson SB (2010) Bacterial competition: surviving and thriving in the microbial jungle. *Nat Rev Microbiol* 8(1):15–25.
31. Macleod SM, Stickler DJ (2007) Species interactions in mixed-community crystalline biofilms on urinary catheters. *J Med Microbiol* 56:1549–1557.
32. Darwin C (1859) *On the origins of species by means of natural selection* (Murray,

London)

33. Burns JH, Strauss SY (2011) More closely related species are more ecologically similar in an experimental test. *Proc Natl Acad Sci U S A* 108(13):5302–5307.

34. Chen SL, et al. (2013) Genomic diversity and fitness of *E. coli* strains recovered from the intestinal and urinary tracts of women with recurrent urinary tract infection. *Sci Transl Med* 5(184):184ra60.

35. Fourcade C, Canini L, Lavigne J-P, Sotto A (2015) A comparison of monomicrobial versus polymicrobial *Enterococcus faecalis* bacteriuria in a French University Hospital. *Eur J Clin Microbiol Infect Dis* 34(8):1667–1673.

36. Ives AR, Carpenter SR (2007) Stability and diversity of ecosystems. *Science* 317(5834):58–62.

37. Gordon DM, Riley M (1992) A theoretical and experimental analysis of bacterial growth in the bladder. *Mol Microbiol* 6(4):555–562.

38. Madersbacher S, et al. (2004) EAU 2004 guidelines on assessment, therapy and follow-up of men with lower urinary tract symptoms suggestive of benign prostatic obstruction (BPH guidelines). *Eur Urol* 46(5):547–554.

39. Boscia J, Kaye D (1987) Asymptomatic bacteriuria in the elderly. *Infect Dis Clin North Am* 1(4):893–905.

40. Flores-Mireles AL, Walker JN, Caparon M, Hultgren SJ (2015) Urinary tract infections: epidemiology, mechanisms of infection and treatment options. *Nat Rev Microbiol* 13(5):269–284.

41. Gleckman R, Blagg N, Joubert DW (1981) Trimethoprim: mechanisms of action, antimicrobial activity, bacterial resistance, pharmacokinetics, adverse reactions, and

therapeutic indications. *Pharmacotherapy* 1(1):14–20.

42. Hitchings GH (1973) Mechanism of action of trimethoprim-sulfamethoxazole--I. *J Infect Dis* 128(Supplement 3):S433.

43. McOsker C, Fitzpatrick P (1994) Nitrofurantoin: Mechanism of action and implications for resistance development in common uropathogens. *J Antimicrob Chemother* 33(suppl A):23–30.

44. Bernier SP, Létoffé S, Delepierre M, Ghigo JM (2011) Biogenic ammonia modifies antibiotic resistance at a distance in physically separated bacteria. *Mol Microbiol* 81(3):705–716.

45. Khanum N, et al. (2012) Influence of pH and temperature on stability of sulfamethoxazole alone and in combination with trimethoprim (co trimoxazole). *Asian J Chem* 24(4):1851.

46. Merton Boothe D (2015) Nitrofurans. *Nitrofurans*:www.merckvetmanual.com/mvm/pharmacology/antibacter.

47. Vega NM, Gore J (2014) Collective antibiotic resistance: mechanisms and implications. *Curr Opin Microbiol* 21:28–34.

48. Kommineni S, et al. (2015) Bacteriocin production augments niche competition by enterococci in the mammalian gastrointestinal tract. *Nature* 526(7575):719–722.

49. Bouatra S, et al. (2013) The human urine metabolome. *PLoS One* 8(9):e73076.

50. Brunet YR, Espinosa L, Harchouni S, Mignot T, Cascales E (2013) Imaging type VI secretion-mediated bacterial killing. *Cell Rep* 3(1):36–41.

51. Xiaokan G, Boedicker JQ (2016) The contribution of high-order metabolic interactions to the global activity of a four- species microbial community. *PLoS Comput Biol* 12(9):e1005079.

52. Nielubowicz GR, Mobley HLT (2010) Host-pathogen interactions in urinary tract infection. *Nat Rev Urol* 7(8):430–441.

53. Kline KA, Fälker S, Dahlberg S, Normark S, Henriques-Normark B (2009) Bacterial adhesins in host-microbe interactions. *Cell Host Microbe* 5(6):580–592.

54. Stacy A, McNally L, Darch SE, Brown SP, Whiteley M (2016) The biogeography of polymicrobial infection. *Nat Rev Microbiol* 14(2):93–105.

55. Costello EK, et al. (2009) Bacterial community variation in human body habitats across space and time. *Science* 326(5960):1694–1697.

56. Brooks T, Keevil CW (1997) A simple artificial urine for the growth of urinary pathogens. *Lett Appl Microbiol* 24(3):203–206.

57. Armbruster CE, Mobley HLT (2012) Merging mythology and morphology: the multifaceted lifestyle of *Proteus mirabilis*. *Nat Rev Microbiol* 10(11):743–754.

58. Flores-mireles AL, Pinkner JS, Caparon MG, Hultgren SJ (2015) EbpA vaccine antibodies block binding of *Enterococcus faecalis* to fibrinogen to prevent catheter-associated bladder infection in mice. *Sci Transl Med* 6(254):1–23.

59. Yoshikawa TT, Guze LB (1976) Concentrations of trimethoprim-sulfamethoxazole in blood after a single, large oral dose. *Antimicrob Agents Chemother* 10(3):462–463.

60. Tsoularis A, Wallace J (2002) Analysis of logistic growth models. *Math Biosci* 179(1):21–55.

61. Meyer PS, Ausubel JH (1999) Carrying capacity: A model with logistically varying limits. *Technol Forecast Soc Change* 61(3):209–214.

62. Kolman C, Girman CJ, Jacobsen SJ, Lieber MM (1999) Distribution of post-void residual urine volume in randomly selected men. *J Urol* 161(1):122–127.

63. Griffiths D, Harrison G, Moore K, McCracken P (1996) Variability of post-void residual urine volume in the elderly. *Urol Res* 24:23–26.

64. Martin LJ, Zieve D, Ogilvie I (2016) MedlinePlus. *Urine 24-hour* medlineplus.gov/ency/article/003425.htm.

65. Lukacz ES, et al. (2011) A healthy bladder: A consensus statement. *Int J Clin Pract* 65(10):1026–1036.

66. Walker-Smith J, Murch S (1999) *Diseases of the Small Intestine in Childhood, 4th Ed* (CRC Press, Oxford).

67. Boron WF, Boulpaep EL (2016) *Medical Physiology, 3rd Ed* (Elsevier Health Sciences).

Acknowledgements

We thank Otto Cordero, Kevin Foster, Eric Kelsic, Marta Lukačišinova, Martin Lukačišin for critical comments on the manuscript, and the whole Bollenbach group, as well as the Genetics group for fruitful discussions. This work was supported in part by Marie Curie Career Integration Grant (CIG) No. 303507, Austrian Science Fund (FWF) standalone grant P 27201-B22, HFSP program Grant No. RGP0042/2013, and NWO Earth and Life Sciences (ALW) VENI project 863.14.015.

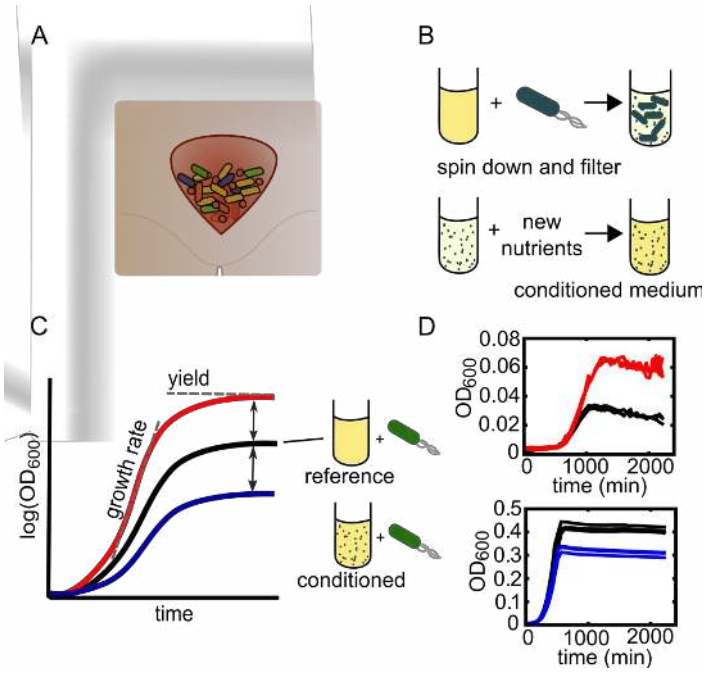

Figure 1. **Quantifying ecological interactions between bacteria isolated from polymicrobial UTIs.** (**A**) Schematic illustrating bladder environment infected with a community consisting of different bacterial species. (**B**) Preparation of conditioned medium for interaction experiments. Bacteria were grown in artificial urine medium (AUM) for 48h, followed by centrifugation and filtration, and replenishment with fresh nutrients. (**C**) Interaction measures from growth in conditioned medium. The growth in the conditioned media is compared to the growth in the reference medium (black) (SI Methods) for each of the 72 isolates. For positive interactions (red), the growth yield in conditioned medium (N_c) exceeds the growth in the reference medium (N_u), $\varepsilon=\log(N_c/N_u) >0$. For negative interactions (blue), the growth in the conditioned medium (N_c) is exceeded by the growth in the reference medium (N_u), $\varepsilon=\log(N_c/N_u) <0$. (**D**) Example

growth curves in triplicate of *Enterococcus faecalis* (top) and *Citrobacter koseri* (bottom) in medium conditioned by *Citrobacter koseri* (color) and reference medium (black). The growth of *Enterococcus faecalis* is positively affected by the conditioned medium (red curve above black curve), whereas *Citrobacter koseri* is negatively affected by medium conditioned by another isolate from the same species (blue curve below black curve).

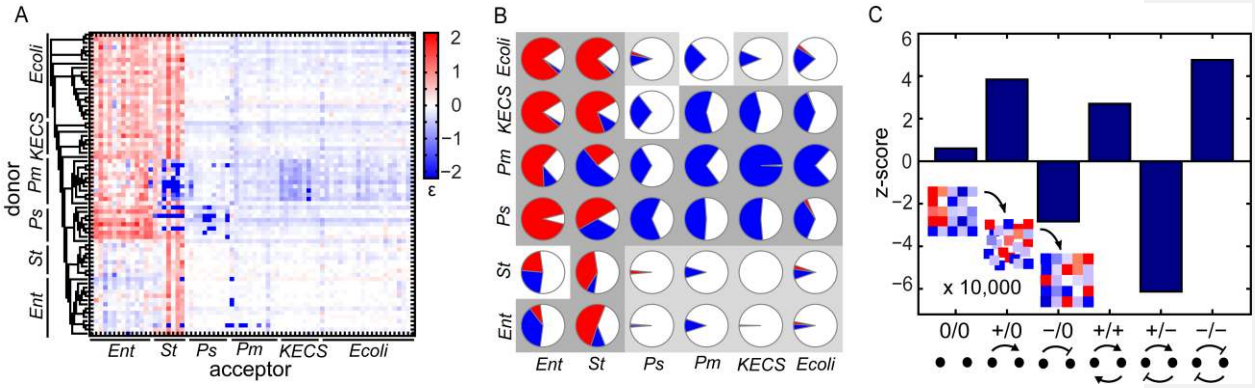

Figure 2. Global UTI interaction network reflects species phylogeny and is enriched for competition, but depleted of exploitation. (**A**) Pair-wise interaction matrix depicting the interactions in yield (maximum reached OD_{600}) of 72 UTI isolates in conditioned medium prepared from these same isolates; the interaction measure is $\varepsilon=\log(N_c/N_u)$ (SI Methods). The acceptors (columns) are grown in the conditioned medium of the donors (rows). Interactions cluster according to phylogeny, as can be seen from the 16S rDNA phylogenetic tree on the left. The isolates are symmetrically ordered on the horizontal and vertical axes. Ent= *Enterococcus* spp (*Enterococcus faecalis* and *E. faecium*), St= *Staphylococcus* spp (*Staphylococcus aureus, S. haemolyticus, S. capitus*), Ps= *Pseudomonas* spp (*Pseudomonas aeruginosa, P. fluorescens*), Pm= *Proteus mirabilis*, KECS= *Klebsiella* spp (*Klebsiella pneumoniae*, *K. oxytoca*), *Enterobacter cloaca*, *Citrobacter koseri*, *Serratia liquefaciens* and *Pantoae* sp4, Ecoli= *Escherichia coli*; one isolate belonging to *Morganella morganii* species is located between Ps and Pm. (**B**) Statistical analysis of phylogenetically clustered interactions. Donors are ordered on the vertical axis, and acceptors on the horizontal axis. Red or blue corresponds to respective positive or negative interactions, dark and light grey background depicts significant over- or underrepresentation of the most prominent interactions compared to randomized matrices,

respectively. A white background depicts non-significant over- or underrepresentation (SI Methods). Statistics on *Morganella morganii* are omitted due to small (N=1) sample size. (**C**) Statistical analysis of all two node-motifs in the measured interaction network. Reciprocal interactions with the same sign (-/- and +/+) and commensalism (+/0) are over-represented, whereas amensalism (-/0) and exploitation (+/-) are depleted. Z-scores were calculated based on the comparison with an ensemble of random networks preserving the degree distribution (inset, SI Methods).

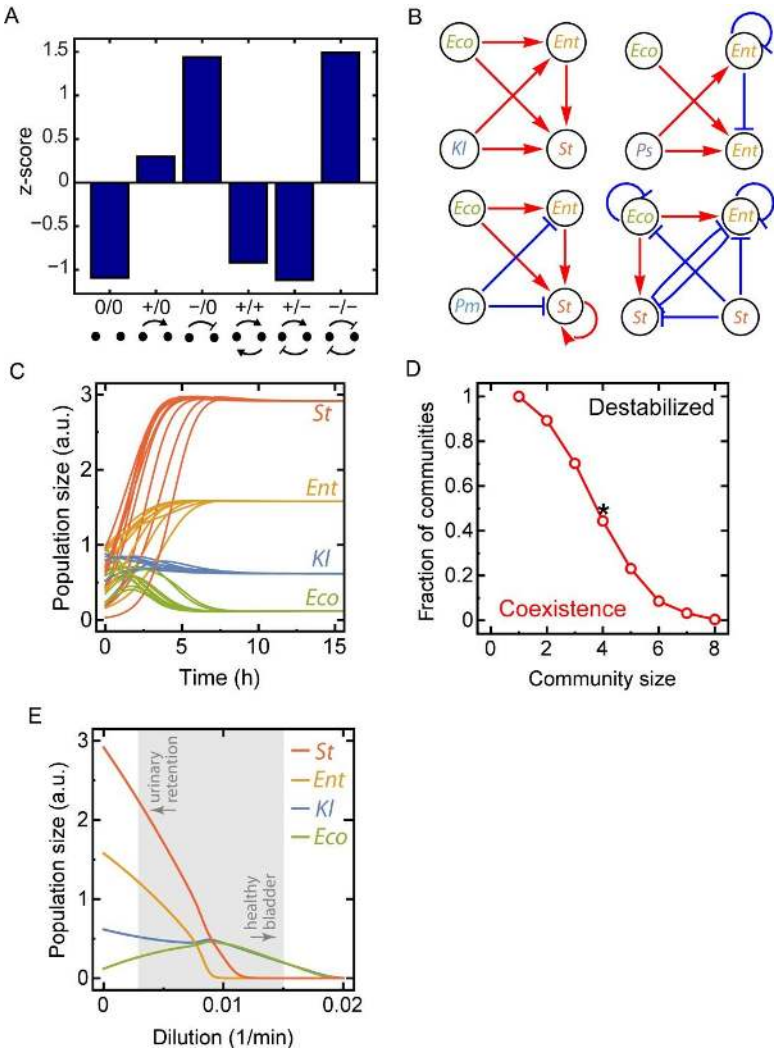

Figure 3. Polymicrobial UTI communities are often ecologically stable and their size is close to the limit of stability. (**A**) Interactions within complete communities compared to interactions in an ensemble of randomized communities (SI Methods). Competitive interactions (-/-) are slightly enriched, while exploitation (+/-) is slightly depleted in communities. No cooperative interactions (+/+) occur in the communities (SI Methods). (**B**) Intra-community microbial interactions in four stable communities. Red: positive interactions, blue: negative interaction.

Abbreviations as in Fig. 2. (**C**) Example population dynamics for one of the stable communities with one fixed point in the absence of voiding. Lines of the same color show independent simulations starting from different initial conditions (SI Methods); the initial population size and inoculation order does not affect the final population size. (**D**) Fraction of stable randomly assembled communities as a function of community size. The stability of the communities drops with increasing community size. The observed typical UTI community size 4-5 is close to the typical size of randomly assembled stable communities. Black asterisk: size and fraction of observed coexisting communities. (**E**) Steady state population size for different UTI species as a function of the effective dilution rate for a stable community (Fig. 3B, SI Methods). The effective dilution rate (mimicking repeated voiding of the bladder) markedly affects the stability of the community. The grey band shows the voiding patterns ranging from a healthy bladder, to a bladder with an increased post-void residual urine volume (Fig. S6, SI Methods).

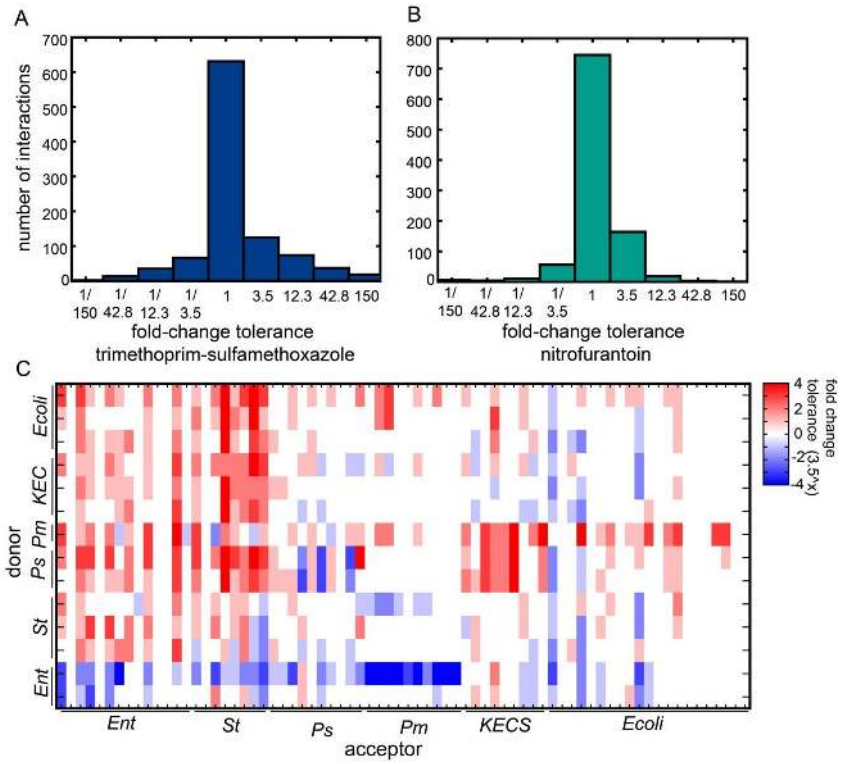

Figure 4. Bacteria in polymicrobial UTIs frequently protect each other from antibiotics.

(**A**) Histogram of the change in tolerance of 72 isolates in 14 conditioned media to the trimethoprim-sulfamethoxazole combination (Fig. S7). (**B**) As A, but for nitrofurantoin. (**C**) Interaction matrix depicting the effect on the tolerance to the trimethoprim-sulfamethoxazole combination of 14 conditioned media on 72 isolates in conditioned medium (SI Methods). Abbreviations as in Fig. 2.

Supplementary Information:

Materials and Methods

Figures S1-S8

Tables S1-S2

Materials and Methods

UTI isolates

Ninety-six isolates from 24 patients (thus 24 host communities) were selected from a previous study (6). Isolates were purified by dilution to extinction on CHROMagar Orientation (CHROMagar) to facilitate the separation. The genus of isolates was confirmed by subsequent Sanger sequencing of the 16S rDNA. Only isolates with verified identity that were able to grow entirely planktonically in AUM were used for the growth measurements. 24 isolates (25%) that did not meet these criteria were excluded. We continued with 72 bacterial isolates from 23 patients, including 8 remaining complete communities isolated from the same hosts. Clonal isolates were pinned on CHROMagar Orientation to reaffirm their identity and frozen as glycerol stocks (v/v 15% glycerol) on 96-well plates.

16S sequencing and phylogeny

Chromosomal DNA from the *Staphylococcus* strains was extracted by suspending a colony in 100 µL of lysis buffer (20 mM Tris-HCl at pH 8.3, 50 mM KCl, 1.5 mM MgCl, 0.5% (v/v) Tween 20, 0.45% (v/v) Nonidet P-40, 0.01% (m/v) gelatin, and 60 µg/mL proteinase K); the mixture was incubated at 55°C for 1 h, followed by 10 min at 95°C. All other strains were lysed by taking a colony, suspending it in 50 µL Milli-Q water, and heating for 10min at 95°C prior to the PCR reaction. PCR amplification was carried out as follows: Initial denaturation at 95°C for 2 min, followed by 35 cycles each of 95°C for 30 s, 51°C for 30s and 72°C for 2 min, and a final elongation step at 72°C for 10 min, using universal 27F-16S (AGAGTTTGATCMTGGCTCAG) and 926R-16S (AAACTYAAAKGAATTGACGG) primers. Each PCR reaction used 25 µL of PCR mix containing: 1x GoTaq Buffer, 0.2 µM of each primer, 2 µL of suspended lysed isolate, 200µM of each dNTP in Milli-Q water. Sequencing of the gene products with above mentioned primers was performed at LGC Genomics and Eurofins. The amplified 16S sequences were aligned using Muscle multiple sequence alignment tool on the www.ebi.ac.uk website. The phylogenetic tree was constructed using the Clustal W tool on the same website, including distance correction.

Artificial urine medium (AUM)

A modified version of the AUM described in (56) was used. The AUM concentration was adapted to achieve planktonic growth of the UTI isolates and to minimize crystal formation in the replenished conditioned medium. The 1x medium contained bacto peptone L37 1.1 g/L (Oxoid), bacto yeast extract 6 mg/L (BD), lactic acid 1.32 mM (Roth), citric acid 2.4 mM, $NaHCO_3$ 30 mM, urea (Roth) 153 mM, uric acid 0.48 mM, creatine 8.4 mM, $CaCl_2$.2HO 0.24 mM, NaCl 108 mM , $FeSO4 \cdot 7H_2O$ 0.006 mM, $MgSO_4.7H_2O$ 12 mM, $Na_2SO_4.10H_2O$ 12 mM (Roth), KH_2PO_4 8.4 mM, K_2HPO_4 8.4 mM, NH_4Cl 30 mM. The AUM medium was buffered with 0.1M pipes (pH 6.5), and 1‰ (v/v)

tritonX-100 was added to prevent clotting, biofilm formation and the deformation of the concave surface of the medium-air interface in the wells of the 96-well plate, which can disturb the OD_{600} measurement. All chemicals were from Sigma unless indicated otherwise.

Spent medium preparation

Isolates were grown for 48h in 40mL 0.75x AUM in vented 50mL culture tubes (TPP) at 30°C and shaken at 200rpm. Cultures were centrifuged at 4,800g for 15 min at room temperature; the supernatant was filtered with 0.2µm filter tops (TPP). The spent medium fraction was replenished with AUM constituents (without sodium chloride), such that the final concentration of constituents in the final "conditioned" medium ranged from 0.6x (for constituents that were consumed in the spent medium) to 1x (for constituents that were not at all consumed in the spent medium) of the concentration in AUM. The pH of the final conditioned media was kept at 6.4-6.5 except for the medium conditioned by *Proteus mirabilis* which ranged from pH 7.3-7.8. This increased pH corresponds to *Proteus mirabilis' in vivo* behavior*;* it hydrolyses urea to carbon dioxide and ammonia, which increases the pH and generates calcium crystals and magnesium ammonium phosphate precipitates (40, 57).

Growth measurements

Each strain was incubated for 36h in one well of a 96-well plate (non-treated transparent flat bottom, Nunc) containing 200 µL of pre-warmed medium. Cultures were inoculated using a replicator (V&P Scientific) transferring ~0.2 µL from a (thawed) overnight culture kept at −80°C (see "UTI isolates" above). The plates were incubated in an automated incubator (Liconic Storex) kept at 30°C, > 95% humidity, and shaken at 720 rpm in aerobic conditions. Optical density at 600 nm (OD_{600}) was measured every ~44 min in a plate reader (Tecan Infinite F500, 5 flashes, 10 ms settle time; filter: D600/20; Chroma). In addition, directly before each measurement, plates were shaken on a magnetic shaker (Teleshake; Thermo Scientific) at 900 rpm for 59s. A customized liquid handling robot (Tecan Freedom Evo 150) was used to automate these experiments and measure over 3,450 growth curves per 36h. The growth rate in exponential phase was quantified from the OD_{600} increase over time by a linear fit of $\log(OD_{600})$ in the range $0.022 < OD_{600} < 0.22$ for all isolates except *Enterococcus* spp; for the enterococci, the range $0.009 < OD_{600} < 0.021$ was used, as these strains typically reach a lower maximum OD_{600} in AUM (enterococci reach OD_{600} ~0.04 in AUM to ~0.1 in some conditioned media, other strains generally reached OD_{600} values of 0.25 to 0.4; this relatively low final OD_{600} of enterococci in non-conditioned AUM corresponds to their poor growth in urine alone (40, 58)). The growth yield (maximum OD_{600} reached) was defined as the mean OD_{600} of the last four measurements. The vast majority of strains reached stationary phase within 20 h, and the OD_{600} largely stayed constant during stationary phase. All experiments were performed in triplicate. Media evaporation from plates and edge effects were virtually undetectable. Directly after each growth experiment the wells were visually inspected for biofilm formation. Isolates that attached to the bottom of the well (observed by scratching each well with a 1 mL pipette tip), clots, or floating biofilms were discarded from the dataset. Biofilm formation occurred primarily for specific isolates, and was genera unspecific. Each 96-well plate contained non-inoculated wells to control for contamination, either in the conditioned medium or during the inoculation procedure. Contamination was negligible.

Analysis of interactions in conditioned medium

Interactions of isolates were defined using the interaction parameter $\varepsilon=\log(N_c/N_u)$, where N_c is the growth yield in condition medium, and N_u the growth in the reference medium (1x AUM concentration). ε is positive ($\varepsilon>0$) if the growth yield (maximum OD_{600}) is higher than that of the reference; negative interactions correspond to $\varepsilon<0$. The level of growth inhibition due to complete niche overlap alone is $\varepsilon\approx\log(0.6)=-0.51$; this value corresponds to the lowest possible concentration of nutrients in the replenished medium. The mean of the triplicate growth measurements was used to calculate the interaction parameter. Unless stated otherwise (e.g. in the theoretical modeling of the community interactions), the conservative thresholds $\varepsilon=\log(0.8)=-0.22$ and $\varepsilon=\log(1/0.8)=\log(1.25)=0.22$ were used for scoring negative and positive interactions, respectively; 95% of the standard deviations around the mean of the triplicate measurements were within the bounds of this 20% threshold. Interactions on growth rate were scored analogously.

Antibiotic tolerance interactions

Isolates were grown in 96-well plates in liquid cultures for 25h. The inoculation and growth procedures were identical to the protocol described above (section "Growth measurements"). The effect of conditioned medium on the action of antibiotics was assessed by scoring the growth in a concentration gradient of two clinically used antibiotics with different modes of action, trimethoprim-sulfamethoxazole and nitrofurantoin (41–43) in the presence and absence of conditioned medium. Five dilutions, with 3.5-fold decrements, and an additional no-drug control were used to determine the maximum antibiotic concentration that could sustain growth. Antibiotic tolerance interactions were scored as the difference in the number of antibiotic concentrations in which growth was observed in conditioned medium versus the AUM (1x concentration) reference. Growth of all isolates (except enterococci, see below) was scored positive if OD_{600} exceeded 0.02 within 25h; growth in *Proteus mirabilis* conditioned medium was conservatively scored positive as (OD_{600}[average last three time points])- (OD_{600}[average first three time points])>0.025 to correct for the increased crystal formation in the medium which affects OD_{600}. As enterococci reach lower final OD_{600} values (see above, section "Growth measurements"), growth was scored as positive if the final OD_{600}>0.01. Antibiotics were added in the conditioned medium just before the start of the tolerance assay, i.e. they were absent during the growth of the donor from which the conditioned medium was produced. The highest concentration of trimethoprim-sulfamethoxazole used was 18.18 µg/mL trimethoprim in combination with 90.90 µg/mL sulfamethoxazole (this 1:5 ratio is in accordance with clinical use (59)), and 200 µg/mL for nitrofurantoin. Trimethoprim was dissolved in 98% ethanol, sulfamethoxazole in acetone, and nitrofurantoin in dimethylformamide (Roth). The effect of the solvents on growth was determined by growing all strains in conditioned and non-conditioned medium with solvent; growth was slightly affected, but never altered the conditioned medium interaction. We used 14 donor strains to generate conditioned medium for the antibiotic tolerance assessment; 9 of these 14 donor strains were part of six of the eight complete communities (section UTI isolates, SI Methods), whereas five were part of incomplete communities.

To assess the effect of neutral ('silent') interactions on antibiotic tolerance, we identified interactions between the 14 donor strains and acceptor strains that were neutral, i.e. between $\varepsilon=\log(0.8)=-0.22$ and $\varepsilon=\log(1.25)=-0.22$, in the

non-antibiotic environment. The interactions between these combinations of donors and acceptor strains quantified in the presence of antibiotics are shown in Fig. S7B,C.

To investigate if the conferred drug tolerance interactions correlated with the sensitivity to the antibiotics of the acceptor isolates in the reference medium, and if the conferred tolerance effect was correlated between both antibiotics, we calculated the Pearson correlation coefficient and corresponding p-values.

To test the community effects on antibiotic resistance (Fig. S7D), only the donor strains derived from a complete community were assessed. These nine donor strains (*Enterococcus faecalis, Staphylococcus aureus, Staphylococcus heamolyticus, E. coli* (three different strains), *Klebsiella pneumonia, Enterobacter cloaca*, and *Proteus mirabilis*) derived from six of the eight complete host communities. To investigate the effect of within and between community effects, we compared the observed fraction of interactions with a certain sign (+/-/0) in the host community to an ensemble of 1,000 randomized communities of isolates derived from those six complete host communities, to calculate z-scores and respective p-values.

Statistical network analysis

The enrichment or depletion of single interactions or two-node subgraphs in the UTI network was quantified with respect to ensembles of randomized networks. Different randomized ensembles were used depending on the specific problem. First, when the distinction between genera was considered (single interactions in Fig. 2B, depletion of -/- and -/0 and enrichment of +/+ and +/0 for different genera) the network of interactions was randomized, conserving the number of positive and negative interactions but not the degree of separate strains. In practice, 10,000 independent random network realizations were assembled and the resulting reference distributions of single interactions or two-node subgraphs were estimated for each genus. Note that the mean of these distributions is genus independent, but the width takes into account the number of strains from a given genus. By comparing estimates from the measured UTI interaction network with the corresponding distributions for the randomized networks, p-values (two-tailed) were calculated as the probability of having a result equal to or more extreme than the actual observation. Second, the enrichment or depletion of two-node subgraphs regardless of genera (Fig. 2C) was estimated with additional constraint imposed; specifically, the degree distribution was conserved. Again 10,000 random network realizations were generated: each network was obtained from the previous one by applying 4×(number of edges)≈8,500 edge swaps independently for random pairs of positive and negative interactions (self-interactions were excluded from the randomization and analysis). The resulting ensemble was used as a reference for quantifying the z-score (and respective p-values) of enrichment or depletion of the two-node subgraphs.

Statistical community analysis

There were 8 complete communities containing 4 strains each (section “UTI isolates”). First, we checked if some pairs of genera occur more often than in the random scenario. As a reference, 10,000 sets with 8 independent 4-strain communities were assembled by randomly sampling strains from the complete communities. Using the obtained distributions, the random expectation and the corresponding p-value (two-tailed) of observing a given pair of genera in the original communities was calculated (Fig. S5A). Second, we checked whether single interactions or two-node subgraphs are significantly enriched or depleted among complete communities. Again 10,000

communities were resampled from the 8 complete communities, but the genera for each community were preserved (e.g. the first community was always composed of *Enteroccocus*, *Staphylococus*, *Klebsiella,* and *E. coli*, and only the corresponding strains changed). The resulting ensemble was used to calculate z-scores and corresponding p-values (two-tailed) for Fig. 3A.

Theoretical model of ecological interactions

We developed a minimal theoretical model describing the ecological interactions that occur between bacteria in a polymicrobial infection. Our model is based on established models (60, 61) of logistic growth in liquid batch culture without spatial structure. The model captures interactions that affect both growth rate and yield independently:

$$\dot{N}_j = N_j g_j \max\left(0,1 + \sum_{j\neq k} a_{jk} N_k\right)\left(1 - \frac{N_j}{\max(0,1+\sum_{j\neq k} b_{jk} N_k)}\right) \qquad (1)$$

Here, N_j is the population size (number of individuals) of strain j and g_j is its growth rate in isolation; N_j is non-dimensionalized so that $N_j = 1$ corresponds to the growth yield at carrying capacity of strain j when grown in isolation. The matrix a_{jk} quantifies the growth rate interactions, i.e. how the growth rate of strain j changes in the presence of strain k (at saturating population size of the latter), relative to its growth rate in isolation g_j: e.g. $a_{jk} = 0$ means that there is no interaction, $a_{jk} = 1$ means that strain j grows twice as fast and $a_{jk} = -1$ means that strain j does not grow at all when strain k is present at its carrying capacity. The latter captures e.g. competition for the same limiting nutrient. Similarly, the matrix b_{jk} quantifies the growth yield change of strain j in the presence of strain k, relative to the growth yield of strain j in isolation. The first max function restricts effective growth rate to be non-negative, whereas the second one ensures that the growth yield does not become negative as a result of the interactions. For simplicity, all interactions are assumed to be additive when more than two strains are present in the community.

If $b_{jk} \equiv 0$ the growth yield for $t \to \infty$ remains $N_j = 1$ as long as the growth rate interactions are sufficiently weak. In general, interactions can, however, lead to very low carrying capacity for the strain j and force the system to the fixed point $N_j = 0$ for $t \to \infty$ (meaning that strain j goes extinct). Importantly, all parameters of this model are fully constrained from our experiments. In particular, the matrices a_{jk} and b_{jk} follow directly from the experimental data shown in Fig. 2A and Fig. S2. The a_{jk} were obtained from the experimentally measured growth rate interactions by simply subtracting 1 from g_c/g_u. The b_{jk} were obtained by subtracting 1 from the measured growth yield interactions N_c/N_u (section "Analysis of interactions in conditioned medium") and linearly rescaling negative b_{jk} to make N_c/N_u=0.6 result in b_{jk} = -1 (to ensure that these values consistently correspond to complete niche overlap). To mimic the regular voiding of the bladder, we further added a dilution term $-DN_j$ on the right hand side of eqn. (1); here D is the effective dilution rate. This term affects the stability properties of the system's fixed points (see main text and Fig. S6).

Theoretical model solutions

The model defined in Eq. (1) is used to determine both the dynamics of the growing bacterial populations and the number of strains in steady-state. In the first case, the forward propagation method was used, i.e. the set of n ODEs

was numerically integrated, where n denotes the number of strains in the community; in practice, the NDSolve function in *Mathematica* was used. By default, the initial population size N_j was assigned a random value from (0, 1] separately for each j (Fig. 3C). To determine the fixed points that correspond to stable coexistence of all species in a given community, Eq. (1) was solved for all steady-states with $N_j > 0$. In practice, this reduces to finding all positive N_j that fulfill either $0 = 1 + \sum_{j \neq k} a_{jk} N_k$ or $N_j = 1 + \sum_{j \neq k} b_{jk} N_k$ for each j separately. Further, for the obtained set of steady state solutions, linear stability analysis was performed to identify only those solutions that are locally stable to fluctuations in population size. 4 out of 8 complete communities had a stable coexistence fixed point. Using the forward propagation method, we found that in 3 of these 4 communities the stable coexistence fixed point is always reached from our initial conditions (typically after several hours); for the one remaining community it is reached in ~85% of cases (at least one strain dies out otherwise).

To determine the typical fraction of stable communities as a function of community size, the strains were randomly assembled into communities of size n = 2,…,8 using the 32 strains that constitute the 8 complete communities. Specifically, 10,000 communities were randomly assembled for n = 2,3,4, and 1,000 communities for n =5,6,7,8. A community was considered stable when at least one stable fixed point with all strains present was found (Fig. 3D).
Next, we studied invasion of the four complete communities at their stable coexistence fixed points. Specifically, the forward propagation method was used with four strains present at their steady-state population size; an invader was added at a small population size of 0.01 at t=0. Each stable community (4 strains) was tested against invasion by any of the 28 strains that were present in the remaining (stable and unstable) complete communities. The outcome of invasions was determined not later than at t=96h; in many cases of failed invasion the invading strain died out almost instantly. The different outcomes of invasion were defined depending on the number of strains that survived with non-zero population sizes (see main text and Table S2).

Finally, the model with dilution term $-DN_j$ added to Eq. (1) was solved by the forward propagation method. The steady state in Fig. S6 was determined after 96h using the population size corresponding to a steady-state with no dilution (D=0) as initial condition.

Estimation of dilution rate

To calculate the range of dilution rates expected for individuals with healthy bladder and for those suffering from urinary retention, we made the following assumptions: (i) the post-void residual urine volume V_R is 5 mL for healthy individuals and 100 mL for those with urinary retention (62, 63); (ii) the total bladder volume V_B = 400 mL in both cases, (iii) there are n voiding events per 24h where $n=(V_L - V_R)/(V_B - V_R)$ depends on the liquid consumption V_L (more precisely, liquid that gets to the bladder); V_L is assumed to be between 1 and 2 L (64–67).

The model in Eq. (1) assumes a continuous dilution rate D, thus we derive D as effective rate equivalent to a series of n discrete voidings per t=24h, that is $(V_R/V_B)^n = \exp(-Dt)$, which results in

$$D = \frac{-n \log(V_R/V_B)}{t} \quad (2)$$

Using the parameter estimates stated above and assuming a high liquid consumption (V_L = 2L), we obtain $D_H \approx$ 0.015 min^{-1} for healthy individuals and $D_R \approx$ 0.006 min^{-1} for those with urinary retention. In the case of lower liquid consumption (V_L = 1L), D_R is reduced to 0.003 min^{-1}. The estimated range of D between 0.003 and 0.015 is rather conservative (Fig. S6); e.g. increasing V_L to 2,500 mL raises D_H to almost 0.02 min^{-1}, whereas an extremely low V_L ≈ 500 mL lowers D_R to 0.001 min^{-1}. In Fig. 3E and Fig. S6 the 'urinary retention' boundary (left side of the grey band) corresponds to a voiding pattern with high urine retention in the bladder (urine residual volume of 100 mL per voiding, 1 L voiding per 24h), the 'healthy bladder' boundary (right side) corresponds to a healthy bladder and voiding pattern (voiding 2L per 24h and residual volume 5 mL).

A

B

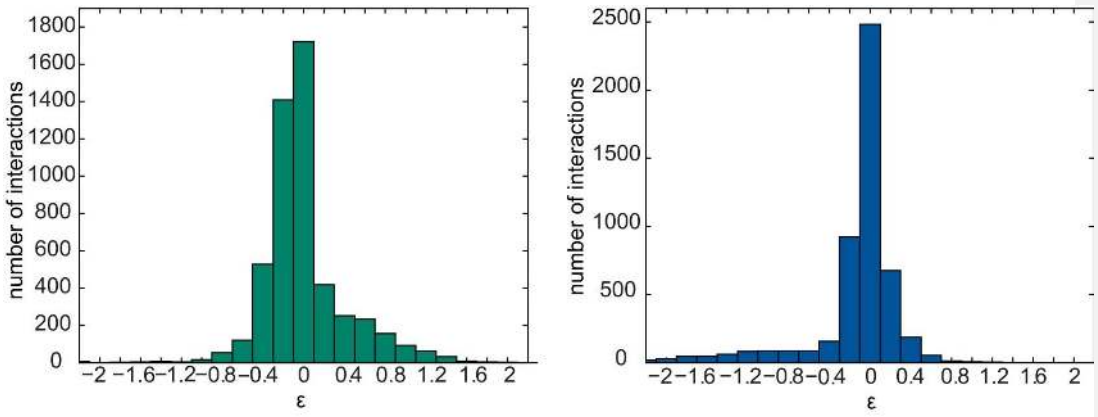

Figure S1. Distribution of all growth interactions.

(**A**) Interactions between UTI bacteria affect the yield (maximum reached OD_{600}). $\varepsilon=\log(N_c/N_u)$; here, N_c and N_u are the growth yield in conditioned and in unconditioned medium, respectively. (**B**) Interactions between UTI bacteria affect the growth rate. $\varepsilon=\log(g_c/g_u)$; here, g_c and g_u are the growth rate in conditioned and in unconditioned medium, respectively.

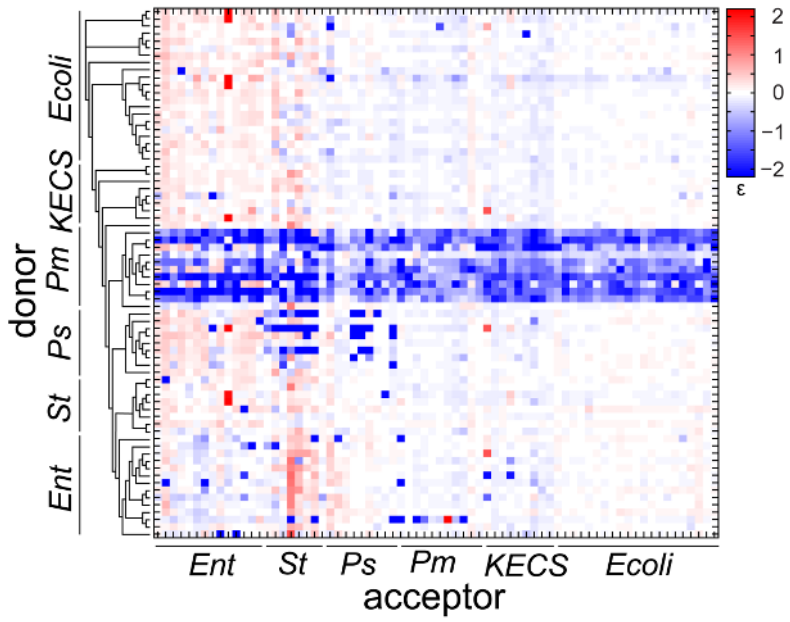

Figure S2. Pair-wise interaction matrix depicting the growth rate interactions of 72 different UTI isolates in conditioned medium prepared from the same isolates.

The acceptors (columns) are grown in the conditioned medium of the donors (rows). Interactions are defined as $\varepsilon=\log(g_c/g_u)$, where g_c and g_u are the growth rate in conditioned and in unconditioned medium, respectively. Interactions cluster according to phylogeny, as can be seen from the 16S rDNA phylogenetic tree on the left. The isolates are symmetrically ordered on the horizontal and vertical axes. Abbreviations as in Fig. 2.

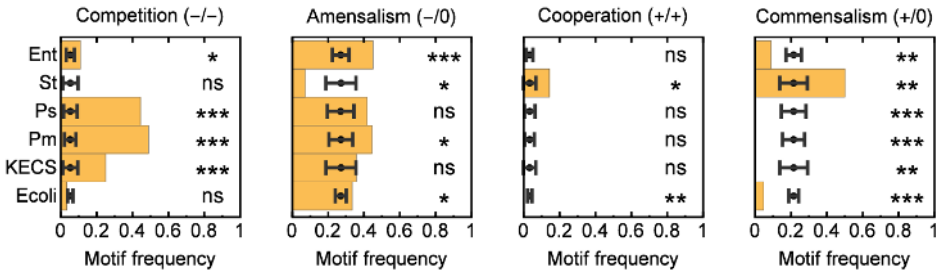

Figure S3. Over/under-representation of mutual interactions within each genus.

The frequency of mutual interactions between strains within the same genus (yellow bars) is compared with the frequency expected for a randomized interaction matrix (black dots; error bars are standard deviation). Competition and amensalism are mostly enriched while cooperation and commensalism are often depleted; *Staphylococcus* is an exception that exhibits the opposite behavior. $p > 0.05$ for "ns" (not significant), $p < 0.05$ for "*", $p < 0.01$ for "**", $p < 0.001$ for "***".

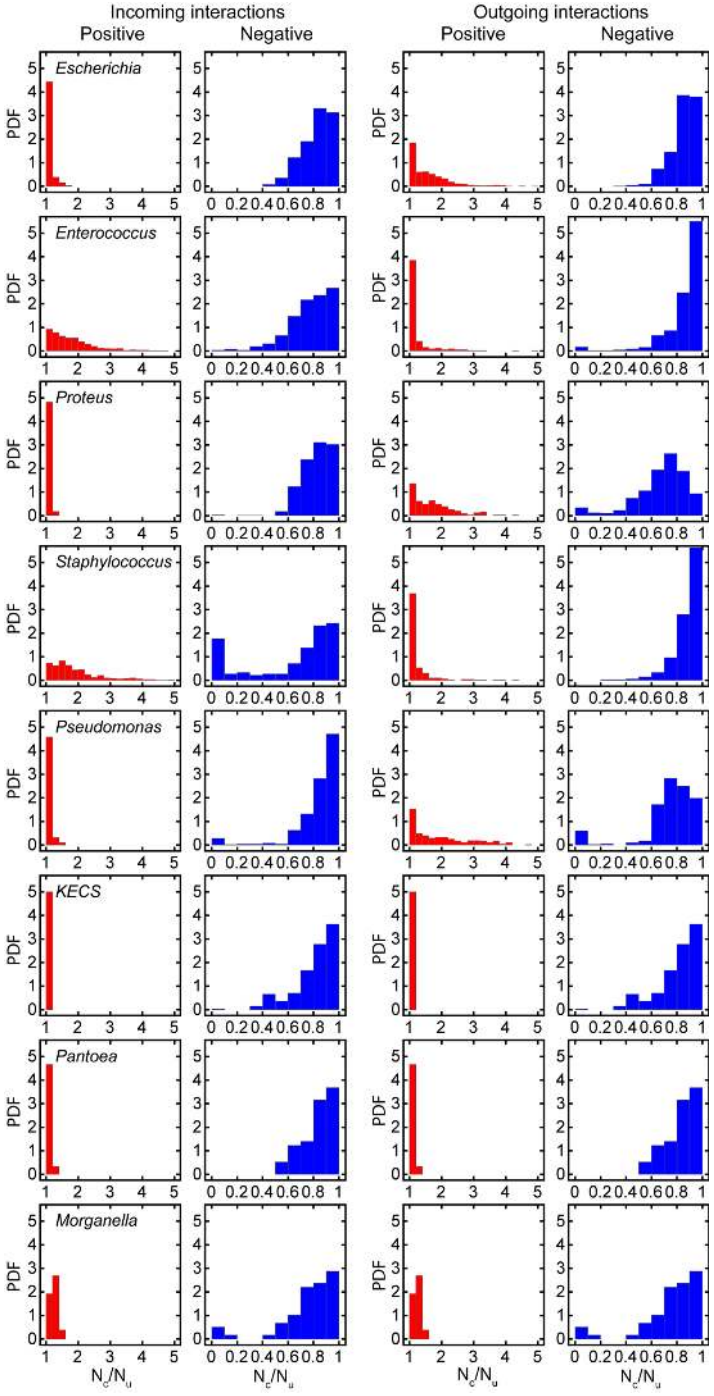

Figure S4. The strength of incoming and outgoing interactions on growth yield, ordered by genera.

Incoming interactions refer to the effect from other genera (donor) on the specific genus (acceptor). Outgoing interactions refer to the effect of the specific genus (donor) on the other genera (acceptor). Negative interactions, $N_c/N_u<1$ ($\varepsilon<\log(1)$), are depicted in blue, whereas positive interactions $N_c/N_u>1$ ($\varepsilon>\log(1)$) are red.

A

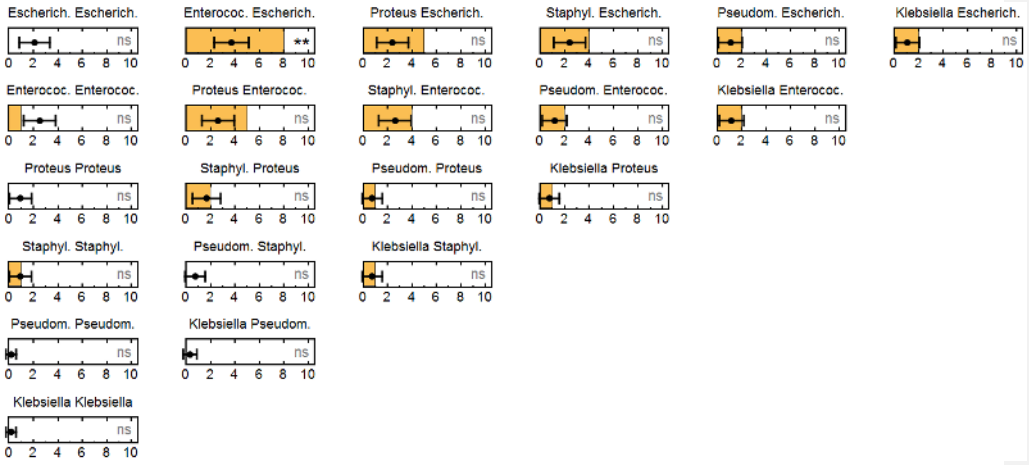

B

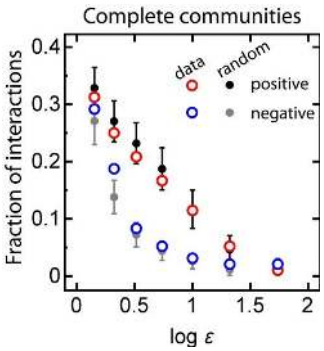

C

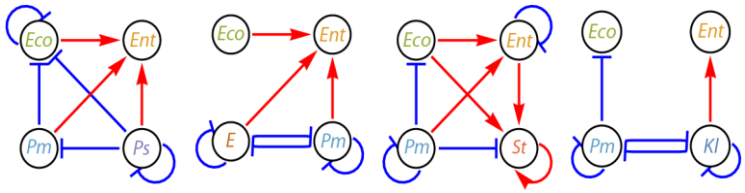

Figure S5. Interactions within UTI communities.

(**A**) The distribution of genera in each community is not random. Specifically, enterococci and *E. coli* occur more frequently together compared to an ensemble of randomly assembled communities of the same size (SI Methods). (**B**) Communities are enriched for negative interactions, whereas postive interactions are slightly depleted. The fraction of interactions with a certain sign (red, blue) are compared to the fraction in an ensemble of randomized communities (black, grey). The x-axis shows the interaction threshold; for all further analyses the threshold level ε=log(0.8)=-0.22 for negative interactions, ε=log(1.25)=0.22 for positive interaction was used; error bars are standard deviations of the fraction of interactions observed in the randomized communities. (**C**) Four complete

unstable communities and their intra-community interactions. Negative interactions (blue), positive interactions (red). Abbreviations as in Fig. 2.

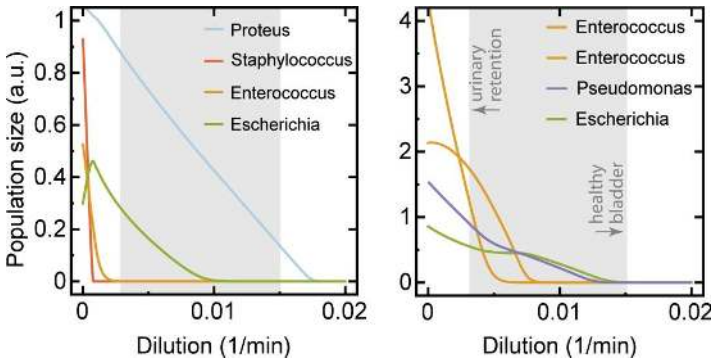

Figure S6. The stability of the UTI communities depends on the effective dilution rate. As Fig. 3E, but for two different host communities. Steady state population size for different UTI species as a function of the effective dilution rate for a stable community. The effective dilution rate (mimicking repeated voiding of the bladder) markedly affects the stability of the community. The grey band shows the voiding patterns ranging from a healthy bladder, to a bladder with an increased post-void residual urine volume. For high effective dilution rates, all UTI community members are washed out. In the lowest dilution regime, the community constituents depend mostly on their intrinsic growth rate and yield and on the ecological interactions among the community members. In the intermediate regime, the dilution rate together with the intrinsic growth rate and yield of each strain determines the population size of the constituents of the community. Note that *E. coli* (the main UTI pathogen in otherwise healthy persons) is consistently among the last two strains that can still persevere at the highest dilution rates.

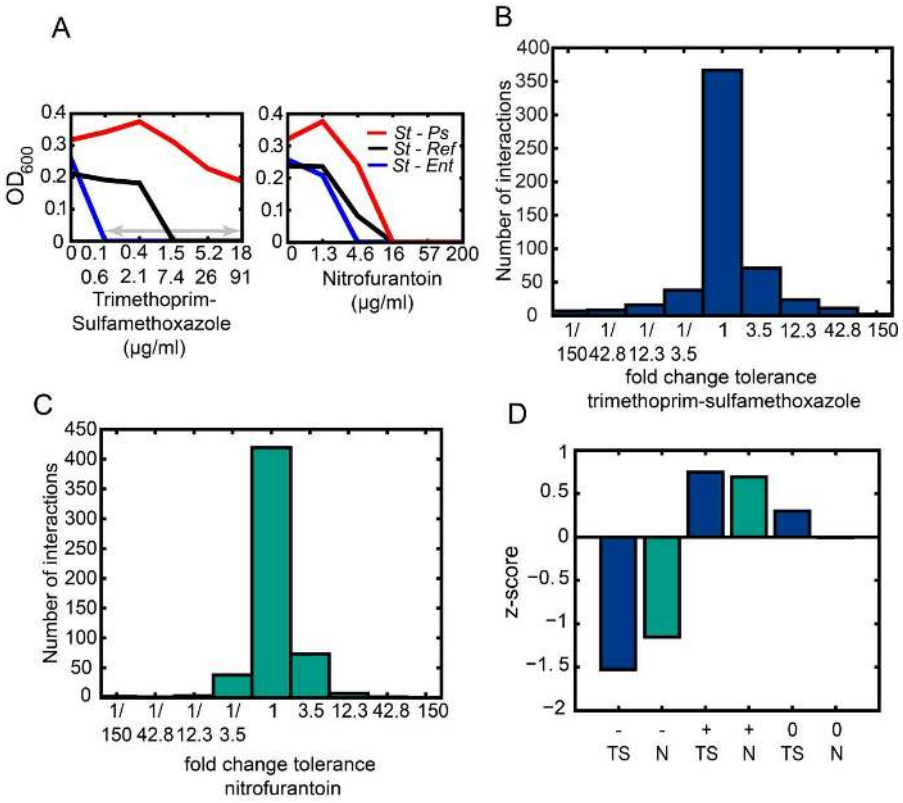

Figure S7. Bacteria in polymicrobial UTIs can protect each other from antibiotics.
(**A**) Bacterial interactions can elicit a change in the dose response curve. The dose response curves (growth yield, OD_{600}, as a function of drug concentration) of *Staphylococcus haemolyticus* for five increasing concentrations of trimethoprim-sulfamethoxazole (left) and nitrofurantoin (right) are shown in the presence and absence of conditioned medium. Black: dose response curve in reference medium (AUM); blue: medium conditioned by *Enterococcus faecalis,* red: medium conditioned by *Pseudomonas aeruginosa*. Arrows point to the change in tolerated concentration antibiotic. (**B,C**) As Fig. 4A,B but only those interactions that are neutral in the absence of antibiotics are depicted. Interactions that are neutral (ε between log(0.8)=-0.22 and log(1.25)=0.22) in the absence of antibiotics can affect the tolerance to trimethoprim-sulfamethoxazole (left) and nitrofurantoin (right). (**D**) Enrichment or depletion of antibiotic tolerance effects within communities. TS=trimethoprim-sulfamethoxazole, N=nitrofurantoin. Interactions between strains within the communities show a depletion of interactions that confer an increased sensitivity to the antibiotics (-), while there is a slight enrichment of protective effects (+), compared to interactions between communities. The fraction of neutral interactions on tolerance (0) does not differ within and between communities.

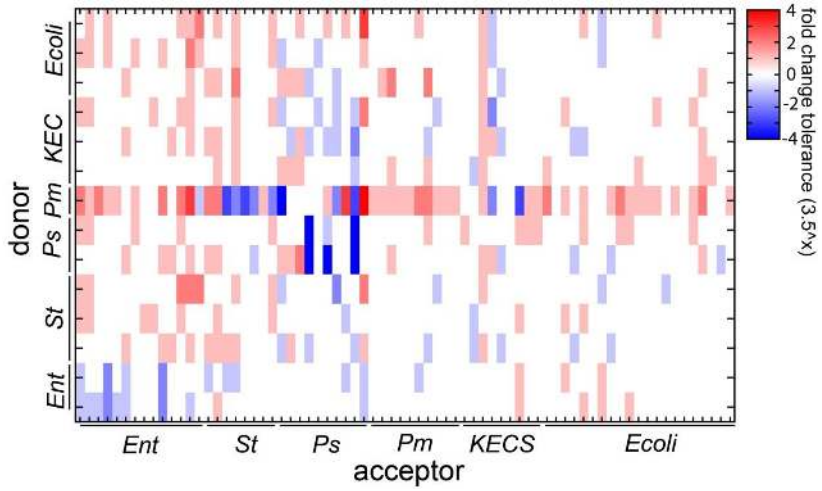

Figure S8. Interaction matrix showing the effect of conditioned medium on the tolerance to nitrofurantoin.

As Fig. 4C, but for nitrofurantoin. Interaction matrix depicting the effect on the tolerance to nitrofurantoin of 14 conditioned media on 72 isolates in conditioned medium (SI Methods). Abbreviations as in Fig. 2.

	Ent Ent	*St St*	*Ps Ps*	*Pm Pm*	*KECS KECS*	*Ecoli Ecoli*
0/0	-0.1134	-0.3970	-0.0102	<-0.0001	0.731	<0.0001
+/0	-0.0018	0.0014	-0.0004	<-0.0001	-0.0016	<-0.0001
+/+	-0.0892	0.0280	-0.5890	-0.4392	-0.7854	-0.0020
-/0	0.0002	-0.0156	0.0794	0.0156	0.4104	0.0498
-/-	0.0436	-0.4284	<0.0001	<0.0001	0.0004	-0.2484
+/-	0.9890	-0.6266	-0.0854	-0.0320	-0.1780	<-0.0001

Table S1. Mutual interactions within each genus. Mutual interactions are generally enriched for competition and amensalism and depleted of cooperation and commensalism; the sole exception is *Staphylococcus* which shows an enrichment of positive interactions. The values shown are p-values, negative values correspond to depletion whereas positive values correspond to enrichment (SI Methods). Abbreviations as in Fig. 2.

Community	Coexist (5 strains present)	Invade & replace a strain	Fail to invade (invader dies)	Invade & destabilize (>1 get extinct)
Ecoli, Ent,Kl,St	0.29	0.43	0.11	0.18
Ecoli,Ent,Ent,Ps	0.68	0.04	0.29	---
Ecoli,Ent,Pm,St	0.39	0.29	0.25	0.07
Ecoli,Ent,St,St	0.43	0.54	---	0.04
average	0.45	0.32	0.16	0.07

Table S2. The fate of the four stable UTI communities upon invasion with a randomly chosen invader. The most common fate of the stable communities when invaded by a randomly chosen invader is that the invader is included in the community. This new community (consisting of 4 plus 1 members) is stable. The next common fates are that one isolate is replaced by the invader, or that the invader goes extinct. In on average 7% of the cases, the invader leads to the destabilization of the community, such that more than one strain goes extinct. Abbreviations as in Fig. 2, and Kl=*Klebsiella*.